

Age of Information Analysis for Multi-Priority Queue and NOMA Enabled C-V2X in IoV

1st Zheng Zhang

School of Internet of Things Engineering
Jiangnan University
Wuxi, China
zhengzhang@stu.jiangnan.edu.cn

2nd Qiong Wu*

School of Internet of Things Engineering
Jiangnan University
Wuxi, China
qiongwu@jiangnan.edu.cn
Corresponding Author

3rd Pingyi Fan

Department of Electronic Engineering
Tsinghua University
Beijing, China
fpy@tsinghua.edu.cn

4th Ke Xiong

School of Computer and Information Technology
Beijing Jiaotong University
Beijing, China
kxiong@bjtu.edu.cn

Abstract—As development Internet-of-Vehicles (IoV) technology and demand for Intelligent Transportation Systems (ITS) increase, there is a growing need for real-time data and communication by vehicle users. Traditional request-based methods face challenges such as latency and bandwidth limitations. Mode 4 in Connected Vehicle-to-Everything (C-V2X) addresses latency and overhead issues through autonomous resource selection. However, Semi-Persistent Scheduling (SPS) based on distributed sensing may lead to increased collision. Non-Orthogonal Multiple Access (NOMA) can alleviate the problem of reduced packet reception probability due to collisions. Moreover, the concept of Age of Information (AoI) is introduced as a comprehensive metric reflecting reliability and latency performance, analyzing the impact of NOMA on C-V2X communication system. AoI indicates the time a message spends in both local waiting and transmission processes. In C-V2X, waiting process can be extended to queuing process, influenced by packet generation rate and Resource Reservation Interval (RRI). The transmission process is mainly affected by transmission delay and success rate. In C-V2X, a smaller selection window (SW) limits the number of available resources for vehicles, resulting in higher collision rates with increased number of vehicles. SW is generally equal to RRI, which not only affects AoI in queuing process but also AoI in the transmission process. Therefore, this paper proposes an AoI estimation method based on multi-priority data type queues and considers the influence of NOMA on the AoI generated in both processes in C-V2X system under different RRI conditions. This work aims to gain a better performance of C-V2X system comparing with some known algorithms..

Index Terms—C-V2X, NOMA, RRI, AoI

I. INTRODUCTION

With the innovation and advancement of IoV technology, the development of ITS has catered to a range of in-vehicle applications such as automated navigation, collision warning, and multimedia entertainment [1]–[6]. Due to the high-speed

mobility of vehicles, ensuring timely access for the required data and content through user requests is crucial [7]–[11], [17]. The traditional request-based approach involves users communicating with the base station, which then accesses the data center to retrieve the requested data [12]–[16]. However, this method suffers from end-to-end delays and limited backhaul bandwidth [18]–[24]. To address these issues, C-V2X proposes an interface called PC5 for communication between autonomous vehicles. PC5 offers two resource allocation methods: Mode 3, where User Equipment (UE) requests time and frequency-domain transmission resources from the eNodeB, and Mode 4, where UE autonomously selects resources without involving the cellular infrastructure. Mode 4 not only eliminates the limited coverage drawback but also minimizes interaction between base stations and vehicles, thereby resolving excessive delays and overhead [25].

In Mode 4, vehicles autonomously select communication resources using the SPS protocol based on distributed sensing. SPS allows vehicles to choose from several standardized message intervals (e.g., 10 Hz, 20 Hz, or 50 Hz). However, this increases the likelihood of collisions when multiple vehicles occupy the same resources with the same message transmission interval, leading to higher BLER [26]. NOMA is a potential solution for C-V2X communication, promising to enhance spectrum efficiency and handle large-scale vehicle communications, mitigating latency and packet reception probability degradation caused by high vehicle density [27]–[29]. Serial Interference Cancellation (SIC) is a well-known Multi-User Detection (MUD) technique used to extract overlapping signals, decoding different power levels of received signals occupying the same resource. High-power signals no longer interfere with other low-power signals after decoding, improving the Signal-to-Interference-plus-Noise Ratio (SINR) of low-power signals, reducing transmission failures due to collisions, and lowering BLER [30]–[33].

This work was supported in part by the National Natural Science Foundation of China under Grant No. 61701197, in part by the National Key Research and Development Program of China under Grant No.2021YFA1000500(4), in part by the 111 Project under Grant No. B12018.

Some studies have examined the effectiveness of NOMA applied in C-V2X. In [34], a NOMA receiver based on Continuous Interference Cancellation (SIC) and Joint Decoding (JD) was proposed, demonstrating its implementation in the current C-V2X communication and its ability to reduce BLER compared to traditional Orthogonal Multiple Access (OMA) methods. In [35], TAKESHI et al. introduced SPS-NOMA based on UpLink Non-Orthogonal Multiple Access (ULNOMA), improving SIC's Signal-to-Noise Ratio (SNR) under broadcast scenarios and alleviating channel congestion. In [36], Utpal et al. proposed a model with a large-scale MIMO Jacobi detection algorithm for PHY layer of C-V2X, enhancing reliability by reducing bit error rate compared to existing PHY layer frameworks. These works demonstrated improvement of NOMA on reliability and transmission delay in the C-V2X system, where reliability and transmission delay were frequently used to assess vehicle communication performance in existing engineering and 3GPP standards.

It is worth noting that these two metrics are often in trade-off, meaning an increase in reliability performance may come at the cost of increased delay. Therefore, a new metric is necessary to comprehensively reflect both reliability and latency performance, such as AoI, where lower average AoI indicates either lower latency with the same reliability or higher reliability with the same delay [37]–[39]. In [40], Peng et al. adopted AoI to evaluate the MAC layer performance of C-V2X sidelink, proposing a Piggyback-based cooperative method for vehicles to inform each other of potential resource occupation, reducing collisions and exhibiting good AoI performance. In [41], Zoubair et al. presented a resource allocation problem based on NOMA, optimizing resource allocation to provide minimum AoI and high reliability for vehicle safety information.

However, the aforementioned studies did not consider the AoI aspect of packet in the queue in C-V2X system. The packet received by the receiver describe the information at the time of packet generation by the transmitter, necessitating consideration of the queuing process. In [42], Akar et al. investigated the freshness of information in IoT-based state update systems using the AoI performance metric. They studied discrete-time servers in multi-source IoT systems, assuming Bernoulli arrivals of information packets and universally distributed discrete phase-type service times across all sources. Their analysis of AoI under various queuing disciplines was formulated in matrix-geometric terms. In [43], Zhang et al. considered a dual-server short-block wireless communication system to ensure real-time delivery of newly generated information at a relatively high update rate to its destination. Information is generated at a relatively high update rate, encoded into two short-block queues, and delivered in real-time through two parallel paths. The study based on the Markov-chain process investigated the AoI performance of the dual-queue system in the presence of block delivery errors.

The AoI of packet generated in the queue is influenced by packet generation rates and service rates, where the service rate in C-V2X depends on the RRI [44]. However, for the

same RRI, while the AoI of transmitter undergoes a short queuing time, the collision probability increases, leading to a potentially large AoI at the receiver [45]. This motivates us to consider this work. In this paper, we propose an AoI calculation approach based on a multi-priority data type queue in C-V2X. We first design a queue model with four types of messages, each with different priorities, allowing the AoI of receiver to better reflect the ability to observe the status of transmitter in a timely manner. We then consider the impact of NOMA on AoI in both processes, calculating AoI for different RRIs, and analyzing effect of multi-priorities queues and NOMA on the C-V2X communication system.¹. The remaining parts of this article are as follows, Section 2 provides a brief introduction to the system model. Section 3 presents a description of the proposed modeling of approach in detail. In Section 4, we present some simulation results, followed by the conclusion in Section 5.

II. SYSTEM MODEL

We consider the system model as shown in Fig. 1. In this model, a cellular-based V2X communication system is with N half-duplex vehicles. In C-V2X Mode 4, all communication resources are in a resource pool, with the smallest unit in the frequency dimension being an RB (Resource Block) with a size of 180 kHz. A sub-channel typically consists of 10 RBs. The time axis is set as a discrete value, with each time slot lasting 1 ms, representing the size of one sub-frame in the resource pool. In C-V2X Mode 4, there are four priority levels of message generating types. When the multi-priority queue is not empty, vehicles will reserve communication resources from the resource pool. The time interval between reserved resources is defined as the RRI, commonly taking values of 20 ms, 50 ms, or 100 ms. The initial value of reserved resources (RC) is defined as $500/RRI + \text{rand}(1000/RRI)$. Moreover, due to half-duplex communication, vehicles cannot receive signals while using communication resources.

We use AoI as the performance metric for this system and calculate the AoI generated in the multi-priority queue and the transmission process. Concerning the AoI in the queue, using communication resources will change the AoI and position of messages in the queue, while not using communication resources will keep them unchanged. Regarding the AoI in the transmission process, upon receiving a signal, the receiver updates its AoI for the transmitter to the AoI of the received signal; otherwise, it increments the AoI by one time slot. For simplicity, the receiver determines whether it receives the signal by comparing the SINR of the received signal with the SINR threshold as the criteria of successful transmission. When C-V2X employs OMA, it will compute SINR, where interferences mainly come from the collisions of other signals. For NOMA mode, SIC (see Eqn.(10) for detail) is used to improve the SINR of low-power signals in collisions, with SINR calculated for received signals in descending order of

¹This paper has been submitted to WCSP. The source code has been released at : <https://github.com/qiongwu86/Analysis-of-the-Impact-of-Multi-Priority-Queue-and-NOMA-on-Age-of-Information-in-C-V2X>

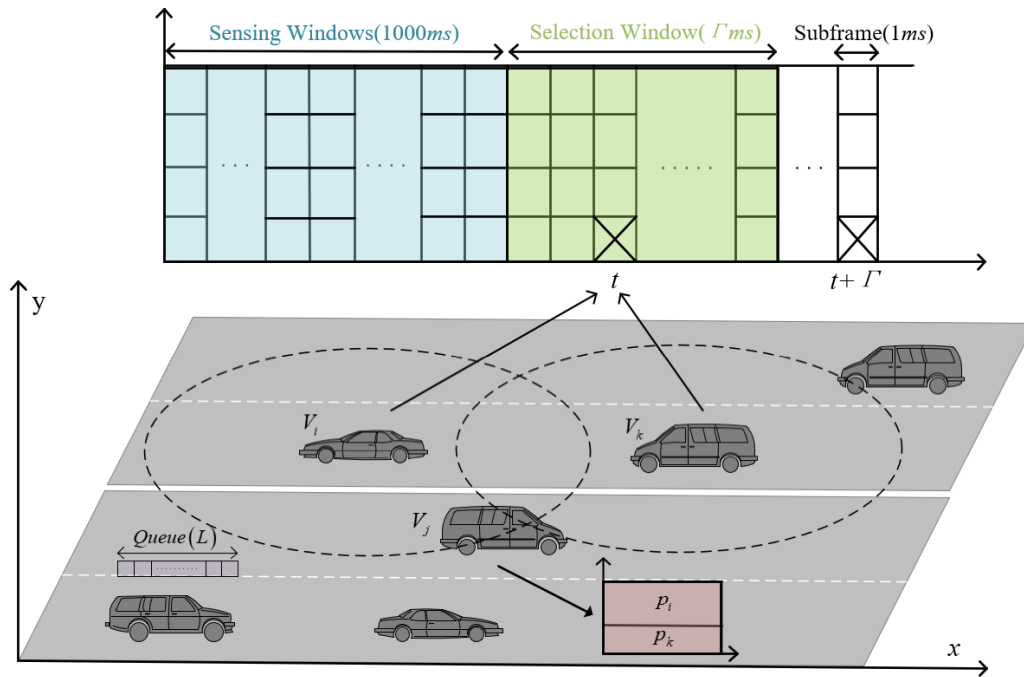


Fig. 1: System Model

their power, where considering only signals with lower power than the current signal as interference. Additionally, in C-V2X, for the same RRI, the AoI in the queue may be very small while the receiver's AoI can be large. To better reflect the improvement of collisions by NOMA, it is necessary to separately calculate the AoI generated in the two processes and analyze the effect of NOMA on the C-V2X communication system.

III. MATHEMATICAL MODEL

In this section, we first establish a computational model to measure the AoI for a C-V2X system with a multi-priority message queue. Subsequently, we propose the use of NOMA based on SIC to improve the AoI in the C-V2X system.

A. AoI in C-V2X

1) C-V2X Queue Model

C-V2X Model 4 consists of four message types with the following priorities: HPD>DENM>CAM>MHD. CAM-type messages are generated periodically, while the other three types are triggered. The generation probability of a new CAM packet is $1/T_c$, where T_c is the fixed packet generation period. The new packet generation probabilities for HPD, DENM, and MHD are represented by a Poisson distribution:

$$P(\text{arr}_{i,n}^t = 1) = \frac{\lambda_n^1}{1!} e^{-\lambda_n} \quad (1)$$

where $n \in \{\text{HPD}, \text{DENM}, \text{MHD}\}$, and λ_n represents the number of packet arrivals for each type of message in a certain time period. For DENM and MHD, the new packets

need to be retransmitted multiple times to ensure successful transmission, and this retransmission process is periodic. Thus, four corresponding First-In-First-Out (FIFO) queues are established based on different signal types. Their queue capacity is L and the queue length is q . When the queues meet $q < L$, corresponding new packets can be added and the same transmission opportunity that leaves the queue can be shared.

The transmission opportunity refers to vehicles can use their own reserved resources, defined as t . At this point, the vehicle transmits messages from different queues based on their priority. When the q of the high-priority message queue is non-zero, the corresponding transmission action s is set to 1, and for other lower-priority queues, s is set to 0. Only when the length q of the high-priority queue is zero, the s of next lower-priority queue can be set to 1. A value of $s = 1$ indicates that the messages in that queue can be transmitted; otherwise, they cannot be transmitted. Therefore, the expression for the transmission action s of the multi-priority queue is:

$$\begin{cases} s_{i,H}^t = 1, s_{i,C}^t = 0 & q_{i,H}^t = 1 \\ s_{i,H}^t = 0, s_{i,C}^t = 1 & q_{i,C}^t (1 - q_{i,H}^t) = 1 \\ s_{i,H}^t = s_{i,C}^t = 0 & \text{otherwise} \end{cases} \quad (2)$$

Due to the sequential prioritization, two priority queues can be used to represent the relationship between the s of different queues. Let $s_{i,C}^t$ represent the transmission opportunity of the HPD queue at the time t , and $s_{i,H}^t$ represent the transmission opportunity of the CAM queue. When the q of all queues are zero, it indicates that no packets can be transmitted, and at this moment, all s are set to 0.

2) Multi-priority queue AoI Model

The cumulative AoI of messages in the queue is a result of the queuing process, defined as the time from packet generation to transmission. Thus, the processing rate affecting the queue length will also influence AoI. The AoI expression for each message in each queue is given by:

$$\varphi_{i,n}^{t+1,b} = \begin{cases} \varphi_{i,n}^{t,b+1} + 1 & s_{i,n}^t = 1 \\ \varphi_{i,n}^{t,b} + 1 & s_{i,n}^t = 0 \end{cases} \quad (3)$$

where n includes the all four queues, $b \in [1, q-1]$ represents the position of the message in the queue at time t for vehicle i , and $\varphi_{i,n}^{t,b}$ denotes the AoI of the message in queue n at position b for vehicle i at time t . When $s_{i,n}^t=1$, the position of all messages in the queue will move except for the first message; When $s_{i,n}^t=0$, all message positions in the queue remain unchanged. Here, $s = 1$ represents the processing rate, and it depends on the 1/RRI in C-V2X. Thus, the RRI will influence the size of AoI.

The cumulative AoI during the communication process can be considered as the time spent to complete the transmission between the receiver and the transmitter, which is influenced by both the transmission delay and the transmission process. Additionally, since the received message reflects the situation at the time of packet generation by the transmitter, the receiver needs to inherit its size to represent the degree of understanding about the transmitter's situation. The AoI expression for receiver j regarding transmitter i is given by:

$$\Phi_{i \rightarrow j}^{t+1} = \begin{cases} \varphi_{i \rightarrow j}^{t,1} + 1 & u_{i \rightarrow j}^t = 1 \\ \Phi_{i \rightarrow j}^t + 1 & u_{i \rightarrow j}^t = 0 \end{cases} \quad (4)$$

where $\Phi_{j,i}^t$ represents the AoI of vehicle j regarding vehicle i at time t , and $u_{j,i}^t$ indicates whether the message is successfully transmitted to j by i . If $u_{j,i}^t=1$, $\Phi_{j,i}^t$ is equal to the $\varphi_{n,i}^{t,1}$ of the highest-priority message in the queue transmitted by vehicle i , plus the transmission delay. If $u_{j,i}^t=0$, $\Phi_{j,i}^{t+1}$ is equal to $\Phi_{j,i}^t$ plus the subframe size. According to Eq.(3) and (4), it can be observed that transmission failure will cause a greater increase in $\Phi_{j,i}^{t+1}$. In C-V2X model 4, the unique way of reserving resources by vehicles means that every transmission failure requires waiting for an RRI interval. The main reason for transmission failure is a low SINR caused by collisions, which can be addressed by NOMA.

B. NOMA in C-V2X

1) Collisions in C-V2X

In C-V2X model 4, vehicles autonomously allocate resources and transmit data in a broadcast manner. When multiple vehicles reserve resources in the neighboring time slots, they may select the same resources. Moreover, due to the broadcast nature, multiple vehicles can simultaneously communicate with the same receiver. This situation leads to collisions when multiple vehicles use the same resources to communicate with the same receiver. According to [46], the non collision probability in C-V2X model 4 can be expressed as:

$$P_{\text{ncol}} \approx \left[1 - \left[1 - \prod_{i=0}^{\Gamma-1} \left(1 - \frac{\pi}{1-\pi i} \right) \right] \frac{1 - P_{\text{rk}}}{\text{CSR} - N_v + 1} \right]^{N_v - 1} \quad (5)$$

where π represents the probability that a vehicle is in the moment of preparing to select a resource, refers to the probability of simultaneously satisfying the three following conditions: the vehicle queue is not empty, the RC is zero, and a new resource is being rescheduled. P_{rk} represents the probability of a vehicle selecting a new resource when the reselection counter resets to zero. CSR represents the total number of resources in the selection window. N_v represents the total number of vehicles. Γ is the size of SW, so CSR follows Γ Increase and increase. However, the variation range of Γ is small, typically being 20, 50, or 100. Thus, when a specific value of Γ is chosen, $\left[1 - \prod_{i=0}^{\Gamma-1} \left(1 - \frac{\pi}{1-\pi i} \right) \right] \frac{1 - P_{\text{rk}}}{\text{CSR} - N_v + 1}$ is a value that changes with the number of vehicles N_v , and as N_v increases, P_{col} also increases. Furthermore, changing the value of Γ as the time interval for vehicles to transmit messages may reduce the collision probability, but it can also increase the waiting time of messages in the queue, leading to a larger AoI. Therefore, considering the impact of collisions, we explore the use of NOMA to mitigate this issue while changing Γ .

2) SINR Calculation

In C-V2X model 4, the size of transmission resources is not fixed. Vehicles calculate the required bandwidth B and the transmission rate threshold R_{th} for successful transmission within one subframe based on the size of the message Q , as expressed by:

$$R_{\text{th}}^t = B_i \log_2(1 + \text{SINR}_{\text{th}}) \quad (6)$$

where $R_{\text{th}} = Q$ because the time taken to complete data transmission for a message must be less than the length of one subframe, i.e., $Q/R \leq 1$. Next, the SINR threshold SINR_{th} is calculated based on the bandwidth and the transmission rate threshold, as shown in the following expression:

$$\text{SINR}_{\text{th}} = 2^{Q_i/B_i} - 1 \quad (7)$$

Due to the varying distances between vehicles at different time instants, the communication experiences different channel impairments, leading to varying communication rates at the receiver. Additionally, since multiple vehicles may use different communication resources within the same subframe, the receiver also receives signals at different rates within different communication resources. If the receiver receives only one signal in a resource, then the SINR between vehicle i and vehicle j at time t is given by:

$$\text{SINR}_{i \rightarrow j}^{t,n} = \frac{p_{i \rightarrow j}^t |h_{i \rightarrow j}^{t,n}|^2}{\sigma^2} \quad (8)$$

where P_i is the transmission power of vehicle i , $|h_{i \rightarrow j}^{t,n}|^2$ is the channel gain between vehicles i and j for resource n , and N_0

is the noise energy. However, due to the half-duplex resource selection scheme in C-V2X, vehicles may select the same resource block when choosing resources, leading to collisions when they use the same resource for transmission. In this case, the wireless information transmission rate is defined as:

$$\text{SINR}_{i \rightarrow r}^{t,n} = \frac{p_{i \rightarrow j}^t |h_{i \rightarrow j}^{t,n}|^2}{\sum_{m \in N_m} p_{m \rightarrow j}^t |h_{m \rightarrow j}^{t,n}|^2 + \sigma^2} \quad (9)$$

where m represents interfering vehicles in the C-V2X scenario, and their transmission energy is denoted as P_m . It can be observed that when multiple vehicles use the same resource, the transmission rate decreases, and if the transmission rate is too low, it may result in transmission failure.

Therefore, to address this issue, we introduce NOMA based on SIC. The receiver sorts the received signals in descending order of received power, considering the maximum received power signal as the target signal and the rest as interference signals. After decoding and removing the target signal, this process is repeated for all signals to compute their SINR. Let $N_k = \{k \in N \setminus i | p_{i \rightarrow j}^t |h_{i \rightarrow j}^{t,n}|^2 > p_{k \rightarrow j}^t |h_{k \rightarrow j}^{t,n}|^2\}$ represent the set of vehicles whose received power is weaker than vehicle i . Then, the SINR for vehicle i is given by:

$$\text{SINR}_{i \rightarrow r}^{t,n} = \frac{p_{i \rightarrow j}^t |h_{i \rightarrow j}^{t,n}|^2}{\sum_{k \in N_k} p_{k \rightarrow j}^t |h_{k \rightarrow j}^{t,n}|^2 + \sigma^2} \quad (10)$$

It can be seen that using NOMA in the event of a collision can reduce the interference on the target signal and increase SINR, thereby reducing the possibility of SINR being lower than the threshold and leading to transmission failure. It is generally believed that $|h_{i \rightarrow j}^{t,n}|^2 = c_{ij} d_{ij}$, c_{ij} represents the coefficient between vehicle i and vehicle j , d_{ij} denotes the distance between vehicle i and vehicle j , and η is the path loss exponent. The value of d_{ij} depends on the positions of vehicles i and j at time t .

3) Vehicle Movement Consider a two-way road with a length of D and $U/2$ lanes in each direction. We establish a coordinate system where the position of vehicle i at time t is defined as (x_i^t, y_i^u) . The origin of the coordinate system is set at the leftmost position of the road, with the x -axis representing the direction of vehicle movement, and the y -axis representing different lanes. Assuming that the vehicle updates its position every very short time, the speed V of vehicle i can be considered constant:

$$x_i^{t+1} = x_i^t + \delta V \tau, x_i^t \in [0, D] \quad (11)$$

where δ represents the direction of vehicle, and set $x_i^0 \in [0, D]$ be the initial position of the vehicle. And y_i^u depends on the lane index $u \in [1, \dots, U]$ of vehicle i , calculated as:

$$y_i^u = u d_y - y_0 \quad (12)$$

where d_y is the width of one lane, and y_0 represents the distance of vehicle i to the edge of the lane. Typically, y_0 is taken as $1/2 d_y$, which is half of the lane width.

IV. NUMERICAL RESULTS AND DISCUSSION

Simulation Tool is MATLAB R2021b. The simulation is conducted based on the existing work with additional modifications. In this section, we present the simulation results for the comparison of AoI in C-V2X under NOMA and OMA, validating the impact of NOMA on AoI in C-V2X.

A. Simulation Settings

According to the C-V2X standard, we use a 10 MHz bandwidth with a total of 50 RBs. The message size is set to 500 Bytes, and QPSK modulation is applied for propagation. The T_C can be an integer multiple of 100 ms between 100 ms and 1 s, typically set to 100 ms. The arrival rates λ_H , λ_D , and λ_M for different message types are set to 0.0001. The T_H and T_D are set to 100 ms and 500 ms, respectively. The K_H and K_D are set to 8 and 5, respectively. The transmission power of all vehicles is uniformly set to 23 dBm, and the speed is set to 120 km/h.

B. Performance Evaluation

Take the mean of $\varphi_{i,n}^{t,b}$ to represent the total AoI of packets in the queue of each vehicle on average, reflecting the queuing situation.

$$\bar{\varphi} = \frac{1}{N_v} \frac{1}{N} \frac{1}{b} \sum_{i=1}^{N_v} \sum_{n \in N} \sum_b^L \varphi_{i,n}^{t,b} \quad (13)$$

where N_v represents the total number of vehicles in the scene, and N is 4, indicating four types of messages. The Δ^t is defined as the average of $\Phi_{i \rightarrow j}^t$ between each pair of vehicles.

$$\Delta^t = \frac{1}{N_v} \frac{1}{N_v - 1} \sum_{j=1}^{N_v} \sum_{i=1}^{N_v-1} \Phi_{i \rightarrow j}^t \quad (14)$$

where, $\Phi_{i \rightarrow j}^t$ represents the AoI between vehicles i and j at time t , which have already computed the AoI between vehicles acting as transmitters and receivers at each moment, taking into consideration the impact of half-duplex communication. Thus, the summation involves calculating the mean AoI between different vehicle pairs i and j . In general, a higher Δ^t indicates a higher number of transmission failures.

Table I presents the communication success rate for different vehicle counts under different values of Γ , which represents the proportion of successfully received messages compared to all received messages. The vehicle density is set at 60 and 100 vehicles/km, and the length of load is set at 500 m. So it can be observed that the success rate is generally higher for 30 vehicles compared to 50 vehicles. This is because an increase in the number of vehicles enhances the probability of reserving resources at the same time, leading to a higher likelihood of resource contention. Furthermore, the success rate at $\Gamma = 20$ ms is consistently lowest. This is because a smaller CSR will result in a higher probability of each resource being reserved by multiple vehicles in scenarios with a greater number of vehicles. Moreover, it is worth noting that, for a given number of vehicles, regardless of the value

TABLE I: Communication success rate in C-V2X

N_v	30			50		
RRI	20	50	100	20	50	100
OMA	0.82891	0.83738	0.91560	0.75367	0.80050	0.85184
NOMA	0.89488	0.93332	0.97274	0.87902	0.92636	0.95356

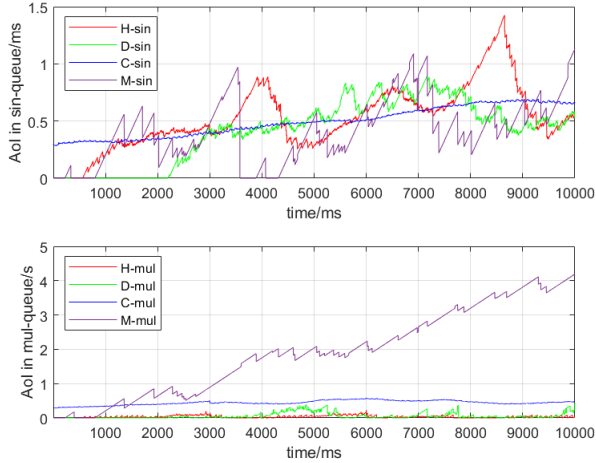


Fig. 2: AvgAoI in different Queues

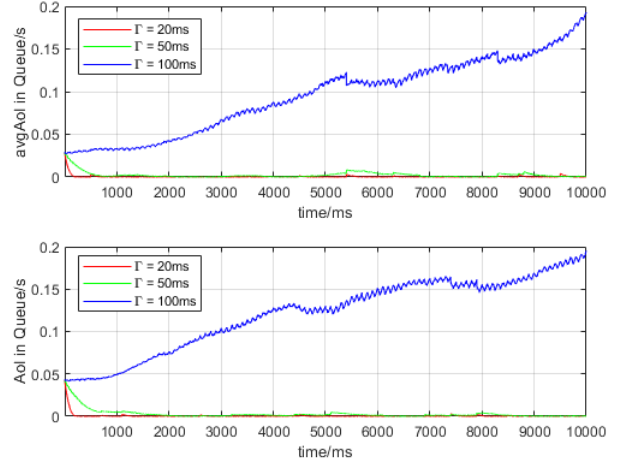


Fig. 3: AvgAoI in Queues

of Γ , employing NOMA technology consistently yields better transmission success rates compared to C-V2X with OMA.

Fig. 2 shows the age variation trend of various messages when the number of vehicles is set to 50 and Γ is set to 100 ms. The upper part of the graph shows the age change of information when a vehicle uses a single queue, while the lower part shows the situation when a vehicle uses a multi priority queue. At this point, the messages in the queue will pile up, leading to an increasing AoI. It can be seen that when there is only one queue, multiple messages queue together, so their overall trend of AoI change is similar. In a multi priority queue, although the probability of generating MHD messages is the lowest, its AoI is the highest due to its lowest priority. So in multi priority queues, the AoI of high priority messages decreases to a certain extent, ensuring the timeliness of high priority messages.

Fig. 3 presents the $\bar{\varphi}$ with different values of Γ when the number of vehicles is 30 and 50, respectively. When Γ is 20 ms, the comprehensive production cycle of various types of packets is close to 100 ms (much larger than Γ), so the queue remains empty for most of the time, the $\varphi_{i,n}^{t,b}$ hardly increases. Similarly, when Γ is 50 ms, the $\bar{\varphi}$ is also relatively small. However, when Γ is 100 ms, which is greater than the production cycle, packets experience more time while waiting in the queue. In addition, it can be observed that when there are more vehicles, the value of $\bar{\varphi}$ increases to a certain extent compared to when there are fewer vehicles.

Fig. 4 shows the Δ^t of 30 vehicles at different Γ . It can be observed that for different Γ , NOMA consistently decreases Δ^t . As shown in Table I, when Γ is 20ms, the collision

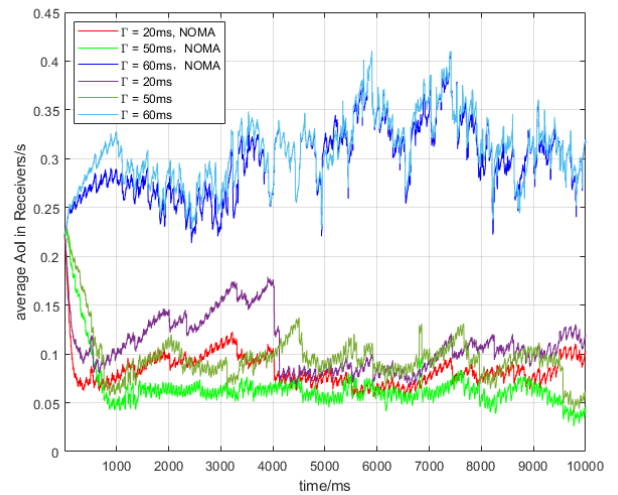


Fig. 4: $N_v = 30$

probability is relatively high, resulting in the message spending the shorter time in the queue, but the information age of the receiving end is not being smaller. By contrast, when Γ is 100 ms, the collision probability is lower. However, due to the accumulation of $\varphi_{i,n}^{t,b}$, it continues to rise and instead becomes the oldest information age among the three situations. When Γ is 50ms, the collision rate is the lowest among the three considered cases, and $\varphi_{i,n}^{t,b}$ does not accumulate, resulting in the lowest Δ^t throughout the entire observation period.

Fig. 5 depicts the Δ^t for 100 vehicles under different values of Γ . A comparison between Fig. 4 and Fig. 5 reveals that

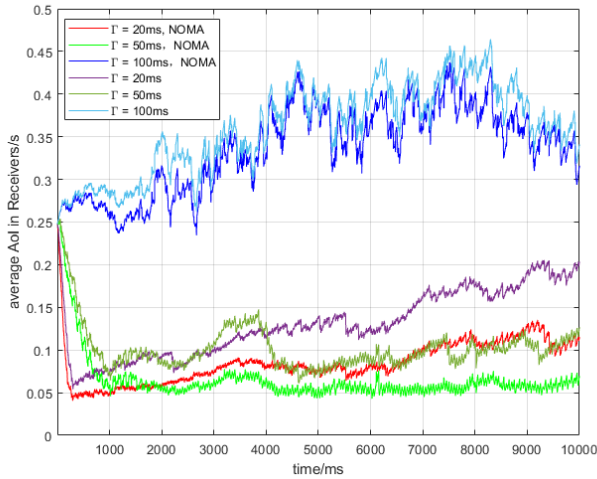


Fig. 5: $N_v = 50$

an increase in the number of vehicles leads to a general upward trend for all cases, which is attributed to the rising collision probability with an increasing number of vehicles. Additionally, the trends in these two cases are similar to those shown in Fig. 4, with the highest information age at $\Gamma=100\text{ms}$ and the lowest information age at $\Gamma=50\text{ms}$. NOMA has positive effects on information age for different Γ .

V. CONCLUSION

This paper considers the mobility of vehicles and analyzes the impact of NOMA on the AoI in different scenarios. Firstly, we propose a novel multi-priority queue AoI calculation model for C-V2X communication. Then, we investigate the improvement in transmission success rate using NOMA based on SIC to observe changes in AoI. The following conclusions are drawn from our analysis:

- Under the same Γ , the collision probability varies with different vehicle counts. Adjusting Γ can reduce collision occurrences, but it must be carefully selected to avoid increased AoI.
- NOMA enhances SINR and reduces the effects of collisions, leading to decreased AoI in various scenarios in C-V2X system.

REFERENCES

- [1] Jing Fan, Shitang Yin, Qiong Wu and Fei Gao, "Study on Refined Deployment of Wireless Mesh Sensor Network," in Proc. of IEEE International Conference on Wireless Communications, Networking and Mobile Computing (WICOM'10), Chengdu, China, Jul. 2010, pp. 370-375.
- [2] Qiong Wu, Hanxu Liu, Cui Zhang, Qiang Fan, Zhengquan Li and Kan Wang, "Trajectory Protection Schemes Based on a Gravity Mobility Model in IoT," Electronics, Vol. 8, No. 148, Feb. 2019.
- [3] Qiong Wu and Jun Zheng, "Performance Modeling of the IEEE 802.11p EDCA Mechanism for VANET," in Proc. of IEEE Global Communications Conference (Globecom'14), Austin, USA, Dec. 2014, pp.57-63.

- [4] Qiong Wu and Jun Zheng, "Performance Modeling of IEEE 802.11 DCF Based Fair Channel Access for Vehicular-to-Roadside Communication in a Non-Saturated State," in Proc. of IEEE International Conference on Communication (ICC'14), Sydney, Australia, Jun. 2014, pp. 2575-2580.
- [5] P. Arthurs, L. Gillam, P. Krause, N. Wang, K. Halder and A. Mouzakis, "A Taxonomy and Survey of Edge Cloud Computing for Intelligent Transportation Systems and Connected Vehicles," in IEEE Transactions on Intelligent Transportation Systems, vol. 23, no. 7, pp. 6206-6221, July 2022, doi: 10.1109/TITS.2021.3084396.
- [6] Qiong Wu, Shuai Shi, Ziyang Wan, Qiang Fan, Pingyi Fan* and Cui Zhang, "Towards V2I Age-aware Fairness Access: A DQN Based Intelligent Vehicular Node Training and Test Method", Chinese Journal of Electronics, vol. 32, no. 6, 2023, pp. 1230-1244.
- [7] Qiong Wu, Shuzhen Nie, Pingyi Fan, Hanxu Liu, Qiang Fan and Zhengquan Li, "A Swarming Approach to Optimize the One-Hop Delay in Smart Driving Inter-Platoon Communications," Sensors, Vol. 18, No. 10, Art. no. 3307, Oct. 2018.
- [8] Qiong Wu and Jun Zheng, "Performance Modeling and Analysis of the ADHOC MAC Protocol for Vehicular Networks," Wireless Networks, Vol. 22, No. 3, Apr. 2016, pp. 799-812.
- [9] Qiong Wu and Jun Zheng, "Performance Modeling and Analysis of IEEE 802.11 DCF Based Fair Channel Access for Vehicle-to-Roadside Communication in a Non-Saturated State," Wireless Networks, Vol. 21, No.1, Jan. 2015, pp.1-11.
- [10] L. Liu, C. Chen, Q. Pei, S. Maharjan and Y. Zhang, "Vehicular Edge Computing and Networking: A Survey," *Mobile networks and applications*, vol. 26, no.3, pp. 1145-1168, 2021.
- [11] Qiong Wu, Wenhua Wang, Pingyi Fan, Qiang Fan, Jiangzhou Wang and Khaled B. Letaief, "URLLC-Aware Resource Allocation for Heterogeneous Vehicular Edge Computing," IEEE Transactions on Vehicular Technology, 2024, doi: 10.1109/TVT.2024.3370196.
- [12] Qiong Wu, Yu Zhao, Qiang Fan, Pingyi Fan, Jiangzhou Wang and Cui Zhang, "Mobility-Aware Cooperative Caching in Vehicular Edge Computing Based on Asynchronous Federated and Deep Reinforcement Learning", IEEE Journal of Selected Topics in Signal Processing, Vol. 17, No. 1, Jan. 2023, pp. 66-81.
- [13] Qiong Wu, Xiaobo Wang, Qiang Fan, Pingyi Fan, Cui Zhang and Zhengquan Li, "High Stable and Accurate Vehicle Selection Scheme based on Federated Edge Learning in Vehicular Networks", China Communications, Vol. 20, No. 3, Mar. 2023, pp. 1-17.
- [14] Dunxing Long, Qiong Wu, Qiang Fan, Pingyi Fan, Zhengquan Li and Jing Fan, "A Power Allocation Scheme for MIMO-NOMA and D2D Vehicular Edge Computing Based on Decentralized DRL", Sensors, Vol. 23, No. 7, 2023, Art. no. 3449.
- [15] Qiong Wu, Siyang Xia, Qiang Fan and Zhengquan Li, "Performance Analysis of IEEE 802.11p for Continuous Backoff Freezing in IoV," Electronics, Vol. 8, No. 12, Art. no. 1404, Dec. 2019.
- [16] S. Wan, J. Lu, P. Fan, Y. Shao, C. Peng and K. B. Letaief, "Convergence Analysis and System Design for Federated Learning Over Wireless Networks," in IEEE Journal on Selected Areas in Communications, vol. 39, no. 12, pp. 3622-3639, Dec. 2021, doi: 10.1109/JSAC.2021.3118351.
- [17] Qiong Wu, Wenhua Wang, Pingyi Fan*, Qiang Fan, Huiling Zhu and Khaled B. Letaief, "Cooperative Edge Caching Based on Elastic Federated and Multi-Agent Deep Reinforcement Learning in Next-Generation Networks," IEEE Transactions on Network and Service Management, 2024, doi: 10.1109/TNSM.2024.3403842.
- [18] Y. Dai et al., "Artificial Intelligence Empowered Edge Computing and Caching for Internet of Vehicles," IEEE Wireless Commun., vol. 26, no. 3, June 2019, pp. 12-18.
- [19] Kan Wang, F. Richard Yu, Lei Wang, Junhui Li, Nan Zhao, Quansheng Guan, Bing Li and Qiong Wu, "Interference Alignment with Adaptive Power Allocation in Full-Duplex-Enabled Small Cell Networks," IEEE Transactions on Vehicular Technology, Vol. 68, No. 3, Mar. 2019.
- [20] Qiong Wu, Siyang Xia, Pingyi Fan, Qiang Fan and Zhengquan Li, "Velocity-Adaptive V2I Fair Access Scheme Based on IEEE 802.11 DCF for Platooning Vehicles," Sensors, Vol. 18, No. 12, Art no. 4198, Dec. 2018
- [21] Qiong Wu, Siyuang Wang, Hongmei Ge, Pingyi Fan, Qiang Fan and Khaled B. Letaief, "Delay-sensitive Task Offloading in Vehicular Fog Computing-Assisted Platoons", IEEE Transactions on Network and Service Management, Vol. 21, No. 2, Apr. 2024, pp. 2012-2026.

- [22] Qiong Wu and Jun Zheng, "Performance Modeling and Analysis of the ADHOC MAC Protocol for VANETs," in Proc. of IEEE International Conference on Communication (ICC'15), London, UK, Jun. 2015, pp. 3646-3652.
- [23] Jing Fan, Qiong Wu and Junfeng Hao, "Optimal Deployment of Wireless Mesh Sensor Networks based on Delaunay Triangulations," in Proc. of IEEE International Conference on Information, Networking and Automation (ICINA'10), Kunming, China, Oct. 2010, pp. 1-5.
- [24] Pingyi Fan, Chongxi Feng, Yichao Wang and Ning Ge, "Investigation of the time-offset-based QoS support with optical burst switching in WDM networks," 2002 IEEE International Conference on Communications. Conference Proceedings. ICC 2002 (Cat. No.02CH37333), New York, NY, USA, 2002, pp. 2682-2686 vol.5, doi: 10.1109/ICC.2002.997330.
- [25] R. Molina-Masegosa and J. Gozalvez, "LTE-V for sidelink 5G V2X vehicular communications: A new 5G technology for short-range vehicle to-everything communications," IEEE Vehicular Technology Magazine, vol. 12, no. 4, pp. 30-39, December 2017.
- [26] 3G Partnership Project. Evolved Universal Terrestrial Radio Access (E-UTRA); Medium Access Control (MAC) Protocol Specification (v14.3.0, Release 14); Technical Report. 36.321; 3G Partnership Project (3GPP): Sophia-Antipolis, France, 2017.
- [27] B. Di, L. Song, Y. Li, and G. Y. Li, "Non-orthogonal multiple access for high-reliable and low-latency V2X communications in 5G systems," IEEE Journal on Selected Areas in Communications, vol. 35, no. 10, pp. 2383-2397, 2017.
- [28] K. Xiong, P. Fan, Z. Xu, H. -C. Yang and K. B. Letaief, "Optimal Cooperative Beamforming Design for MIMO Decode-and-Forward Relay Channels," in IEEE Transactions on Signal Processing, vol. 62, no. 6, pp. 1476-1489, March 15, 2014, doi: 10.1109/TSP.2014.2298380.
- [29] X. Chen, J. Lu, P. Fan and K. B. Letaief, "Massive MIMO Beamforming With Transmit Diversity for High Mobility Wireless Communications," in IEEE Access, vol. 5, pp. 23032-23045, 2017, doi: 10.1109/ACCESS.2017.2766157.
- [30] Y. Zhang, K. Peng, Z. Chen, and J. Song, "SIC vs. JD: Uplink NOMA techniques for M2M random access," Communications (ICC), 2017 IEEE International Conference on, pp. 1-6, 2017.
- [31] J. Liu, K. Xiong, D. W. K. Ng, P. Fan, Z. Zhong and K. B. Letaief, "Max-Min Energy Balance in Wireless-Powered Hierarchical Fog-Cloud Computing Networks," in IEEE Transactions on Wireless Communications, vol. 19, no. 11, pp. 7064-7080, Nov. 2020, doi: 10.1109/TWC.2020.3007805.
- [32] R. Jiang, K. Xiong, P. Fan, Y. Zhang and Z. Zhong, "Power Minimization in SWIPT Networks With Coexisting Power-Splitting and Time-Switching Users Under Nonlinear EH Model," in IEEE Internet of Things Journal, vol. 6, no. 5, pp. 8853-8869, Oct. 2019, doi: 10.1109/JIOT.2019.2923977.
- [33] Y. Guo, K. Xiong, Y. Lu, D. Wang, P. Fan and K. B. Letaief, "Achievable Information Rate in Hybrid VLC-RF Networks With Lighting Energy Harvesting," in IEEE Transactions on Communications, vol. 69, no. 10, pp. 6852-6864, Oct. 2021, doi: 10.1109/TCOMM.2021.3098030.
- [34] Z. Situ, I. W. -H. Ho, Y. Hou and P. Li, "The Feasibility of NOMA in C-V2X," IEEE INFOCOM 2020 - IEEE Conference on Computer Communications Workshops (INFOCOM WKSHPS), Toronto, ON, Canada, 2020, pp. 562-567, doi: 10.1109/INFOCOMWKSHPS50562.2020.9163009.
- [35] T. Hirai and T. Murase, "Performance Evaluation of NOMA for Sidelink Cellular-V2X Mode 4 in Driver Assistance System With Crash Warning," in IEEE Access, vol. 8, pp. 168321-168332, 2020, doi: 10.1109/ACCESS.2020.3023721.
- [36] U. K. Dey, R. Akl and R. Chataut, "Performance Improvement in Cellular V2X (C-V2X) by Using Massive MIMO Jacobi Detector," 2022 IEEE 19th International Conference on Smart Communities: Improving Quality of Life Using ICT, IoT and AI (HONET), Marietta, GA, USA, 2022, pp. 122-127, doi: 10.1109/HONET56683.2022.10019065.
- [37] S. Kaul, R. Yates, and M. Gruteser, "Real-time status: How often should one update?" in Proc. IEEE INFOCOM, Mar. 2012, pp. 2731-2735.
- [38] Y. Ge, K. Xiong, Q. Wang, Q. Ni, P. Fan and K. B. Letaief, "AoI-minimal Power Adjustment in RF-EH-powered Industrial IoT Networks: A Soft Actor-Critic-Based Method," in IEEE Transactions on Mobile Computing, doi: 10.1109/TMC.2024.3356229.
- [39] H. Zheng, K. Xiong, P. Fan, Z. Zhong and K. B. Letaief, "Age of Information-Based Wireless Powered Communication Networks With Selfish Charging Nodes," in IEEE Journal on Selected Areas in Communications, vol. 39, no. 5, pp. 1393-1411, May 2021, doi: 10.1109/JSAC.2021.3065038.
- [40] F. Peng, Z. Jiang, S. Zhang and S. Xu, "Age of Information Optimized MAC in V2X Sidelink via Piggyback-Based Collaboration," in IEEE Transactions on Wireless Communications, vol. 20, no. 1, pp. 607-622, Jan. 2021, doi: 10.1109/TWC.2020.3027353.
- [41] Z. Mlika and S. Cherkaoui, "Deep Deterministic Policy Gradient to Minimize the Age of Information in Cellular V2X Communications," in IEEE Transactions on Intelligent Transportation Systems, vol. 23, no. 12, pp. 23597-23612, Dec. 2022, doi: 10.1109/TITS.2022.3190799.
- [42] N. Akar and O. Dogan, "Discrete-Time Queuing Model of Age of Information With Multiple Information Sources," in IEEE Internet of Things Journal, vol. 8, no. 19, pp. 14531-14542, 1 Oct. 1, 2021, doi: 10.1109/JIOT.2021.3053768.
- [43] Z. Zhang, X. Zhu, Y. Jiang, J. Cao and Y. Liu, "Closed-Form AoI Analysis for Dual-Queue Short-Block Transmission with Block Error," 2021 IEEE Wireless Communications and Networking Conference (WCNC), Nanjing, China, 2021, pp. 1-6, doi: 10.1109/WCNC49053.2021.9417272.
- [44] G. P. Wijesiri N.B.A., J. Haapola and T. Samarasinghe, "A Markov Perspective on C-V2X Mode 4," 2019 IEEE 90th Vehicular Technology Conference (VTC2019-Fall), Honolulu, HI, USA, 2019, pp. 1-6, doi: 10.1109/VTCFall.2019.8891331.
- [45] M. Gonzalez-Martín, M. Sepulcre, R. Molina-Masegosa and J. Gozalvez, "Analytical Models of the Performance of C-V2X Mode 4 Vehicular Communications," in IEEE Transactions on Vehicular Technology, vol. 68, no. 2, pp. 1155-1166, Feb. 2019, doi: 10.1109/TVT.2018.2888704.
- [46] G. P. Wijesiri N.B.A., J. Haapola and T. Samarasinghe, "A Discrete-Time Markov Chain Based Comparison of the MAC Layer Performance of C-V2X Mode 4 and IEEE 802.11p," in IEEE Transactions on Communications, vol. 69, no. 4, pp. 2505-2517, April 2021, doi: 10.1109/TCOMM.2020.3044340.